Resonant inelastic diffraction of low energy electrons

A. A. Moskalev and V. S. Tsoĭ

Institute of Solid State Physics, USSR Academy of Sciences
(Submitted 26 December 1986)
Zh. Eksp. Teor. Fiz. **93**, 330–342 (July 1987)

We have experimentally detected and investigated a new, resonant type of inelastic diffraction of low-energy electrons. Characteristics include resonant dependence on the energy of electrons incident upon a surface, nearness of the direction of inelastically diffracted low-energy electrons to that of elastically diffracted electrons, and smaller angular width than for elastic diffraction. We propose a model of resonant inelastic diffraction of low-energy electrons in which an incident electron is trapped in a surface state, followed by emission of both a surface plasmon and an electron into the vacuum.

INTRODUCTION

The phenomenon of inelastic diffraction of low-energy electrons (ILEED) is manifested by the appearance of a set of sharp maxima, the ILEED peaks, in the angular distribution of the electron flux reflected with low energy losses ($\lesssim 50$ eV) from a surface.[1] ILEED is known to be describable (see Ref. 2 and the literature cited therein) by a two-step model,[3] in which an incident electron takes part in two successive processes, elastic diffraction and energy loss. There are two possibilities, with the energy loss preceding the diffraction (LD-process) or vice versa (DL-process).

Elastic diffraction of low-energy electrons (ELEED) is a thoroughly studied phenomenon which leads to sharp maxima, the ELEED peaks, in the angular distribution of the electron flux reflected with no energy loss. In the two-step model, the ILEED peaks occur in the vicinity of the ELEED peaks as a result of the marked forward elongation of the differential cross section during the energy loss process.

A new type of inelastic diffraction, resonant ILEED, was reported in Ref. 4. Besides phenomena explainable in terms of the two-step model, the authors observed in Ref. 4 a resonant dependence of the ILEED peak intensities on the energy E_p of the electron beam incident on the surface, and a narrowing of these peaks relative to the corresponding ELEED peaks. In order to explain the observed features, a model of resonant ILEED was proposed in Ref. 4, according to which an electron incident on the sample is trapped in a surface state under the resonance conditions described by McRae,[5] followed by emission of a surface plasmon and ejection of the electron into the vacuum.

The present paper is a continuation of Ref. 4, and contains a description of the measurement methodology, experimental data obtained in a test of the proposed model, and their analysis.

EXPERIMENTAL METHODOLOGY

A monochromatic, collimated beam of electrons was directed at the (111) surface of an atomically pure monocrystal of antimony, which was maintained in ultrahigh vacuum. That part of the surface from which reflection took place was located at the center of a system of four concentric grids and a luminescent screen, which is the standard four-grid ELEED analyzer. The two outermost grids were grounded, while the two inner grids were fed a retarding voltage E_r. Electrons reflected from the surface traveled along the local normal to the grids, so that only electrons with energies greater than E_r passed through the grids. The resulting brightness of the luminescent screen was proportional to the electron flux striking it. Using an image dissector, a fast-acting transmitting television tube, operating in photon-counting mode, we measured the brightness distribution $I(\theta_0,\varphi_0,E_r)$ at the luminescent screen in the vicinity of the selected ELEED peak for a given E_r with θ_0 and φ_0 respectively the polar and azimuthal reflection angles. For $E_2 > E_1$, the difference $I(\theta_0,\varphi_0,E_1) - I(\theta_0,\varphi_0,E_2)$ determines the angular distribution of the reflected flux of electrons which have lost an amount of energy between $E_p - E_2$ and $E_p - E_1$ in exciting the crystal. The choice of E_1 and E_2 makes it possible to distinguish among excitation processes, and in particular to identify ILEED involving excitation of a surface (volume) plasmon. We also measured the E_p-dependence of the peak intensities.

The measurements were made at room temperature, using a high-speed computer-controlled system for gathering and processing LEED data.[6] We used a Reber high-vacuum system with a slow-electron diffractometer, Auger and mass spectrometers, and a sample preparation chamber. The surface to be studied was obtained by cleaving, cleaned by heating; its chemical purity was monitored by taking Auger spectra (see Ref. 6). The working vacuum was kept at $\sim(1–2)\cdot 10^{-9}$ Torr.

The small recorded ILEED signal represented the difference between two large signals (the ILEED peaks are typically an order of magnitude weaker than the corresponding ELEED peaks), so the role played by signal noise and drift during the measurement increased significantly. Because of surface structure defects, thermal vibrations of the atoms, and various inelastic reflection processes not contributing to ILEED, the angular distribution of the reflected electron flux shows a background with a smooth angular dependence, which makes it more difficult to detect ILEED peaks. During the measurements the ELEED peak was seen to shift by angles θ_0 and φ_0 of tenths of a degree as E_r was varied, as a consequence of which there typically remained a difference in $I(\theta_0,\varphi_0,E_1) - I(\theta_0,\varphi_0,E_2)$ between the shifted and unshifted ELEED diffraction maxima, containing a peak and a "dip" of the same order of magnitude as the ILEED peak. The magnitude of the shift is a sensitive function of the position of the sample in the analyzer, and in-

 0038-5646/87/070190-08$04.00

creases with decreasing $E_p - E_r$. This shift is due to the deviation of the electron trajectory from the direction of the retarding-grid electric field. Slowing of an electron in the intergrid gap increases this deviation, thereby determining the change in motion of the electron along the tangent to the grids during the time of flight in the intergrid gap, i.e., the shift of the point of electron impact on the luminescent screen (peak shift).

To reduce the noise, provision was made for signal integration. In order to reduce the effect of signal-strength drift on the shape of ILEED peaks, about a hundred signal-strength distributions were averaged over angle during the measurement process, with a time constant of 0.01 sec per point, or ~ 5 sec for one distribution. With this integration, drift had no effect on the shape of each distribution, but the overall integration time was considerable. Following integration, the noise was smoothed by averaging intensity values adjacent in angle. The angular scanning step size was $\sim 0.5°$, and the angular resolution of the device was $\sim 1°$, i.e., smoothing had a negligible effect on angular resolution. To reduce drift of the incident beam current, the cathode of the electron gun was heated carefully. Typical measurement errors in the ILEED peak intensities, due to system noise and current drift, were $\lesssim 5\%$ and $\lesssim 10\%$ respectively (an order of magnitude larger than for ELEED peaks).

The scanning region in the vicinity of the ELEED peak was rectangular, and was so chosen that its boundary did not intersect the diffraction peak. The shape and strength of the measured peaks were then practically independent of the size of the scanning region. Since measurements were made over a wide range of energies (for different peaks), the ratio of the peak height to the background level also varied over a wide range: for the strongest peaks, the background was $\lesssim 0.1$ of the ELEED peak heights, and for the weak peaks, the background was several times the peak height. After integrating the signal and smoothing the noise, the background was subtracted as follows. The intensity distribution in the scanning region was represented in the computer as a matrix, θ_0 and φ_0 monotonically varying over the rows and columns. For every row, we calculated a linear function passing through the values at the edges, and this function was subtracted from each element along the row. The same process was then carried out with the columns.

Diffraction peak intensities, particularly for resonant ILEED peaks, show a strong variation when the incident beam deviates from the normal to the surface by an angle $\theta < 1°$. As a rule, normal incidence ($\theta = 0°$) was used, and the incident beam was precisely aligned to the normal with an acuracy $\sim 0.2°$. Proof of alignment was equality of the E_p-dependences of ELEED peaks equivalent by virtue of surface symmetry (for more detail see Ref. 6).

The θ_0-component of the shift in the ELEED peak as E_r varies can be eliminated by repositioning the sample along the axis of the beam, but the shift cannot be eliminated completely, except in special cases. The determining factors here are due to design features of the analyzer: its nonspherical grids, imprecision in the setup of the sample, grids, and electron beam, the finite diameter of the electron beam, and so forth. In our measurements, the shift in the ELEED peaks was compensated; following subtraction of the background, the maxima of the peaks in the subtracted distributions coincided. The ILEED peak is small, so adding it to the ELEED peak leaves the location of the maximum in the distribution $I(\theta_0, \varphi_0, E_r)$ practically unchanged. Coincidence of the maxima corresponds to coincidence of the locations of the ELEED peak. As a result, the difference $I(\theta_0,\varphi_0,E_1) - I(\theta_0,\varphi_0,E_2)$ determines the angular intensity distribution of reflected electrons which have lost energy in the range from $E_p - E_2$ to $E_p - E_1 (E_2 > E_1)$. A criterion of the correctness of this procedure is the absence of a "dip" next to the peak in the resulting angular distribution.

A number of control measurements were made to establish the sensitivity of the mathematical processing, equipment adjustment, and the state of the surface. For the (03) peak at $E_p = 306$ eV, we measured the dependence of the angular distribution of elastically and inelastically reflected electrons on the position of the sample along the axis of the incident beam. The sample was displaced by $+2.5$ mm along the axis near the center of the analyzer, the change in θ_0 then being 1°, which exceeds the ELEED peak shifts observed when E_r is varied. As a result, we detected a correlated change of approximately 10% between the intensities of the ILEED and ELEED peaks over the whole range of displacements. This change in ILEED peak intensity is close to the measurement error due to current drift (see above). The direction and shape of the peaks were independent of the position of the sample on the axis. It proved to be possible to choose conditions under which there was no shift in the ELEED peak (peak (03), $E_p = 306$ eV) as E_r varied, and the determination of the angular distribution of the inelastically reflected electrons did not require shift compensation for the ELEED peak. In that instance, the peaks were practically the same as those obtained by the foregoing procedure with the ELEED peak shift produced by a change of sample position in the analyzer. With no smoothing, the angular distributions have approximately three times the noise (nine values of intensity, adjacent in angle, take part in the smoothing), and the peak heights increase somewhat. When the background was approximated by a linear function over the whole measurement range of $I(\theta_0,\varphi_0,E_r)$ in θ_0 and φ_0, the backgroud irregularities in the angular distributions were smaller than the ILEED peak amplitudes, and showed no sharp peaks or "dips" in intensity. It has been observed experimentally that the shape and location of ELEED and ILEED peaks correspond to the symmetry of the surface: equivalent peaks have the same shape and the location of the peaks corresponds to a threefold symmetry axis C_3, with three mirror planes passing through C_3. For the (03), $E_p = 306$ eV peak, it has been shown that the observed ILEED features are independent of the choice of which part of the surface is used for diffraction, of the sample heating between two measurements, and of the duration of surface irradiation by the incident electron beam prior to measurement.

RESULTS

Energy spectrum of reflected electrons. In our experiments, the delay curves $I(E_r)$ were measured under the following conditions: For the electron beam incident normal to the surface ($\theta = 0°$) the recording directions in the neighborhood of the (02) and (03) ELEED peaks were at the peak maximum; a "slope" of the peak (at the maximum of the ILEED peak for the (02) case); a background region

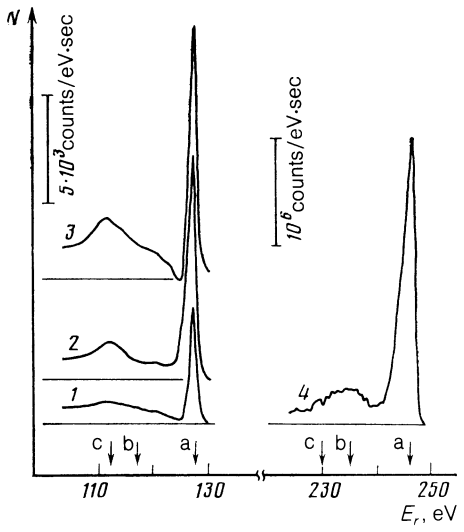

FIG. 1. $N(E)$ in the vicinity of the ELEED (02) peak ((1) In the background region near the peak; (2) maximum of the diffraction peak; (3) "slope" of the peak), and (4) at the maximum of the ELEED (00) peak. Arrows indicate (a) E_p; (b) $E_p - E_{s,\mathrm{pl}}$; (c) $E_p - E_{b,\mathrm{pl}}$. The zero levels of N are shown.

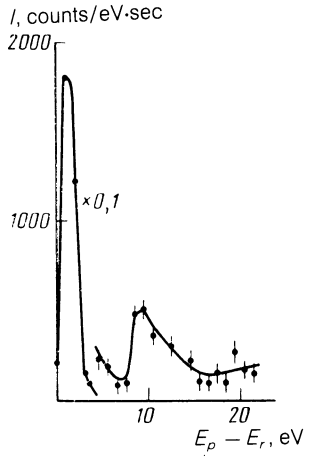

FIG. 2. E_r-dependence of the amplitude of the peak in the angular distribution of reflected electrons with energies in the range from E_r to $(E_r + 1)$ eV for the (10) peak, $E_p = 39\frac{3}{4}$ eV. The left-hand part of the curve is shown at a reduced vertical scale.

near the peak at $E_p = 128$ eV in the case of the (02) and $E_r = 306$ eV for the (03) peak. For the incidence angle $\theta = 60°$, the recording direction was at the maximum of the specular peak, with $E_p = 246$ eV. Curves giving the energy distribution of reflected electrons $N(E_r)$ were obtained by differentiating $I(E_r)$ with respect to E_r. According to Ref. 7, the energy of a bulk plasmon in antimony is $E_{b,\mathrm{pl}} = 16$ eV, and the corresponding energy of a surface plasmon is $E_{s,\mathrm{pl}} = E_{b,\mathrm{pl}}/\sqrt{2} \approx 11$ eV. At normal incidence, all of the curves for $N(E_r)$ (Fig. 1) are similar in appearance: a clearly delineated elastic peak at $E_r = E_p$, a prominent broad peak displaced from E_p and $E_{b,\mathrm{pl}}$, and a very weak feature at $E_p - E_{s,\mathrm{pl}}$. The strongest peak at $E_r - E_{b,\mathrm{pl}}$ (curve 3 of Fig. 1) is seen at the ILEED diffraction peak with excitation of a volume plasmon. The amplitude differences in the elastic peak are small in the curves of Fig. 1 for all recording directions, including that of the ELEED maximum peak, due to the high background level, which is markedly different for different recording directions, and it is relatively small for a given value E_p of the ELEED peak amplitude. At $\theta = 60°$, there is a significant change in the behavior of $N(E_r)$: the strong maximum is displaced from the vicinity of $E_p - E_{s,\mathrm{pl}}$ (curve 4, Fig. 1).

A peak was observed in the angular distribution of the reflected electrons with energies in the range from E_r to $(E_r + 1)$ eV; in order to obtain this distribution in a rectangular scanning field in the vicinity of the ELEED peak, we measured $I(\theta_0,\varphi_0,E_r)$ at values of E_r from E_p to $(E_p - 20)$ eV in 1-eV steps ($E_p = 128$ eV and 306 eV). The dependence of the peak amplitude on E_r was similar in appearance to curve 3 of Fig. 1—a high maximum at $E_r = E_p$ (ELEED peak), a pronounced maximum at $E_r = E_p - E_{b,\mathrm{pl}}$ (ILEED peak), and a weak maximum at $E_r = E_p - E_{s,\mathrm{pl}}$ (ILEED peak).

As a rule, in order to record the ILEED peaks due to plasmon excitation, taking acount of the energy spectrum of the reflected electrons, we measured $I_{s,\mathrm{pl}} = I(\theta_0,\varphi_0,E_p - 13) - I(\theta_0,\varphi_0,E_p - 6)$ and $I_{b,\mathrm{pl}} = I(\theta_0,\varphi_0,E_p - 20) - I(\theta_0,\varphi_0,E_p - 13)$ for the surface and volume plasmons respectively. The ELEED peaks were recorded by measuring the angular distribution I_a of the quasielastically reflected electrons. When necessary, measurements were carried out within a narrower window in E_r, requiring considerably more computation time because of the relatively high magnitude of the noise resulting from a weak signal. In particular, such measurements were made for the ILEED (10) peak, which is large in the narrow energy range $\Delta E_k \approx 2$ eV (the maximum amplitude of the peak is at $E_k = 39\frac{3}{4}$ eV; see below), and are shown in Fig. 2. These data indicate that the energy of a surface plasmon in antimony excited via resonant ILEED is (9.5 ± 1) eV, which differs considerably from the value $E_{b,\mathrm{pl}}/\sqrt{2} \approx 11$ eV.

E_p-dependence of ILEED *for normal surface incidence of electron beam.* Because of equipment limitations, measurements of the E_p-dependence were made in the energy ranges 30–250 eV and 290–350 eV. In those energy ranges out of the total range indicated in which no ELEED peaks could be detected, no ILEED peaks were observed either. Among the observed ILEED peaks due to plasmon excitation, one series was satisfactorily described within the scope of the two-step model. There the E_p-dependence of the amplitude of the peaks (Fig. 3) indicates that when bulk plasmons are involved, both LD and DL processes occur: the peak in curve 3 of Fig. 3 is broadened toward larger E_p as compared with the peak showing the E_p-dependence of the amplitude of the ELEED peak (curve 1). Only the DL process occurs when a surface plasmon is involved: the E_p-dependence of the height of the ILEED peak (curve 2) is a copy of the corresponding function for the ELEED peak. Besides the indicated ILEED peaks, however, others have been detected with a surface plasmon participating (resonant ILEED peaks), the existence of which is clearly in conflict with the two-step model, in particular the nature of the E_p-dependence of the amplitude at resonance. It is important that the resonance of these ILEED peaks in E_p is narrower than for the ELEED peaks, which also have resonant behavior in E_p, with the width of the resonance depending of E_p and increasing with increasing E_p. In plots 1 and 2 of Fig.

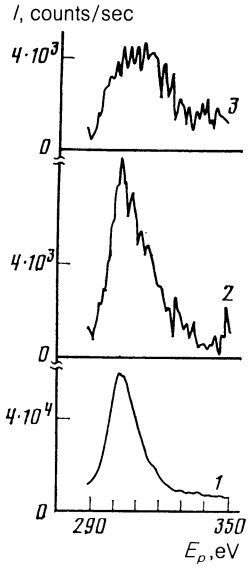

FIG. 3. E_p-dependence of the amplitude of (03) peaks: (1) ELEED; (2) ILEED with surface plasmon; (3) ILEED with volume plasmon.

4, we show I_a and $I_{s,pl}$ for the ELEED and ILEED (10) peaks at $E_p = 39\frac{3}{4}$ eV. For small changes in E_p on either side of $39\frac{3}{4}$ eV, the ILEED peak disapears, while the ELEED peak height changes monotonically with E_r. Plots 3 and 4 of Fig. 4 give I_a and $I_{s,pl}$ for the (10) peaks at $E_p = 38$ eV; the ILEED peak is absent. Table I gives indices for the resonant ILEED peaks and energy values $E_p = E_k$ at which they reach maximum amplitude. For $E_p \lesssim 90$ eV, the resonant ILEED peaks are only seen in a neighborhood $\Delta E_k \approx 2$–3 eV about the corresponding E_k, and their intensity falls to zero toward the edges of this interval. In the range $E_p \sim 100$–200 eV, resonant ILEED peaks are seen over the wider interval $\Delta E_k \approx 3$–6 eV. At high energies, ILEED peaks are observed over a wide range of E_p, but near resonance ($\Delta E_k \approx 10$ eV) they are narrowed (see below). For the (30) return at $E_p = 308$ eV, a narrow peak was observed to occur on a broad "pedestal," with the peak having a resonant dependence on E_r in a neighborhood $\Delta E_k \approx 10$ eV. At energies E_k, the amplitude of resonant ILEED peaks was higher than off resonance.

Detailed measurements of the behavior of the amplitude of the resonant ILEED peak as a function E_p were carried out for the (10) peak in the vicinity of $E_p \sim 40$ eV. The (10) peak was chosen for the following reasons: for that peak, only resonant ILEED takes place, and ΔE_k is a minimum, with the resonance being clearly defined. The results are presented in Fig. 5, where it can be seen that there are two resonant values of the energy, $39\frac{3}{4} \pm 1/4$ eV and $42\frac{1}{4} \pm 1/2$ eV.

Angular distribution of reflected electrons. We have measured the angular distribution of inelastically reflected electrons $I_{s,pl}$ with extensive signal integration. Two features were detected in the angular distribution of electrons producing the resonant ILEED peaks. First, the direction of diffraction in a resonant ILEED peak is practically the same as that of the corresponding ELEED peak over the entire energy range. Second, the resonant ILEED peaks have a smaller angular width that the corresponding ELEED peaks. These features are illustrated in Figs. 4 and 6. They are readily apparent at energies $E_p \lesssim 220$ eV, when the directions of the two-step and resonant ILEED peaks can be distinguished (in plots 2 and 5 of Fig. 6, the resonant ILEED peak is on the left). The two-step ILEED peaks have a larger angular width than the ELEED peaks, while that of the resonant ILEED peaks is smaller (Figs. 4,6). At high energies, the difference in angular width between the resonant ILEED and ELEED peaks is diminished, which is partly due to the coincidence in direction of the resonant and two-step ILEED peaks. We have evidently only been able to distinguish between these ILEED returns at high energy for the (30) peak at $E_p = 308$ eV (see above), where the narrow resonant peak is the resonant ILEED peak, and the broad "pedestal" is the two-step ILEED peak. For the (03) peak at

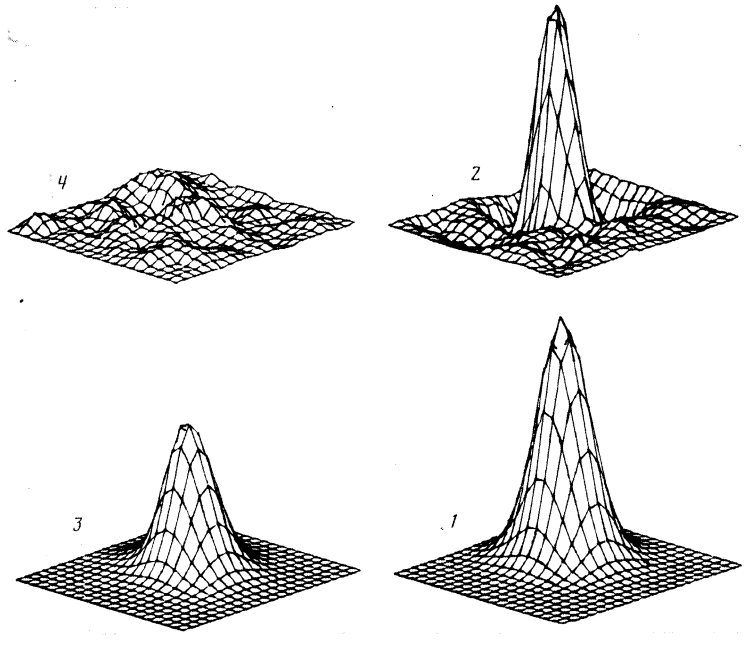

FIG. 4. Structure of (10) ELEED (curves 1,3) and surface-plasmon ILEED (curves 2,4) peaks; $E_p = 39\frac{3}{4}$ eV (curves 1,2) and $E_p = 38$ eV (curves 3,4). The momentum P_r is plotted on the horizontal axes, with one division representing 0.03 Å^{-1}. The intensity (vertical) scale is arbitrary, and is magnified by a factor of 10 for ILEED.

TABLE I.

E_k	Peak	E_k	Peak	E_k	Peak
$39\frac{3}{4}$	(10)	154	(02)	306	(03)
$42\frac{1}{4}$	(10)	160	(11)	308	(30)
77	(11)	164	(11)		
92	(11)	164	(20)		
116	(02)	180	(11)		
118	(20)	191	(02)		
126	(02)	210	(30)		
130	(20)	251	(30)		

$E_p = 306$ eV, the resonant nature of the ILEED is manifested only by a narrowing of the peak to $\Delta E_k \approx 10$ eV. We have used as a parameter of the angular width of the peak the ratio of the "volume" of the peak to its height for a fixed base area. Narrowing was characterized by the ratio r of the width parameter of the ELEED peak to the width parameter of the ILEED peak. For resonant ILEED peaks with a variety of E_k, the value of r lay in the range 1.1 to 2.0. For two-step ILEED peaks, $r \approx 0.4$–0.8.

ILEED *dependence on electron beam angle of incidence at the surface*. The second decisive condition in observations of resonant ILEED peaks, besides the narrow energy range ΔE_k, is the normal incidence of the electron beam at the surface (in contrast to two-step ILEED peaks, for which the angle of incidence does not play an important part). In Fig. 6, we show measurements for the (02) peak with $E_p = 116$ eV and two directions of electron-beam incidence, namely normal to the surface, and inclined $\sim 1°$ to the plane passing through the direction of the $(2\bar{1})$ ELEED peak. It can be seen from Fig. 6 that deviation of the beam from normal incidence results in a drastic reduction in the amplitude of the peak (the angle of incidence shows a resonance). Because of the abrupt drop in amplitude of the resonant ILEED peak for off-normal incidence of the incident beam and equipment limitations, we were unable to make any quantitative measurements of the dependence of E_k on the angle of incidence θ; only qualitative data were obtained. The measurements were carried out for the (10) peak ($E_k = 39\frac{3}{4}$ eV at $\theta = 0°$). This choice was made because it gave the minimum value of ΔE_k and the highest resonant ILEED intensity, with no nonresonant ILEED. Tilting the beam away from the normal in the plane passing through the (01) peak direction by $\pm 2°$ reduced the resonant energy by 5 ± 2 dB.

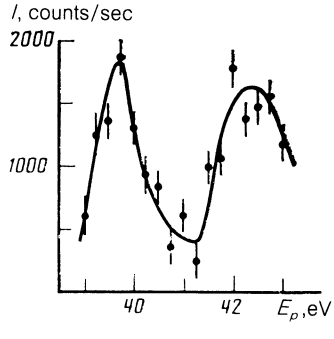

FIG. 5. E_p-dependence of the amplitude of the (10) peak for resonant ILEED.

DISCUSSION

The two-step ILEED diagram for normal electron incidence at the surface producing a surface plasmon is shown in Fig. 7. Energy is conserved upon diffraction, and so is the component of the electron momentum parallel to the surface, modulo the reciprocal lattice vector **G**. Energy and momentum are conserved during production of the plasmon. Since the momentum of a surface plasmon is directed along the surface, the LD process involving such a plasmon is forbidden. The DL process takes place in the following manner. After elastic diffraction, an electron incident on the surface with momentum P_0 and energy E_p will have momentum $P_\pm$; it then produces a surface plasmon with momentum

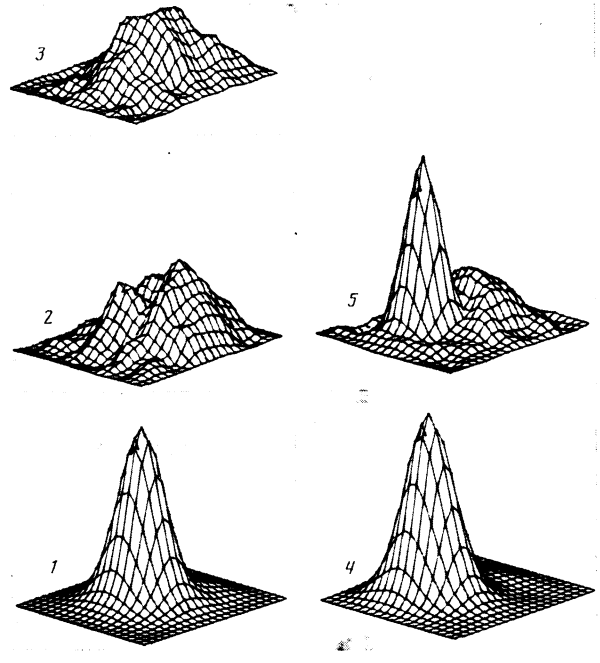

FIG. 6. Structure of the (02) ELEED peaks (plots 1,4), ILEED peaks involving a surface plasmon (plots 2,5), and ILEED peaks involving a bulk plasmon. For 1, 2, and 3, the incident beam is inclined to the normal to the surface; for 4 and 5, the two coincide, and $E_p = 116$ eV. The momentum P_τ is plotted along the horizontal axes, with one division equal to 0.05 Å^{-1}, and the coordinate origin is displaced to the right of the ELEED peak. For the ILEED peaks, the vertical scale is magnified by a factor of ten.

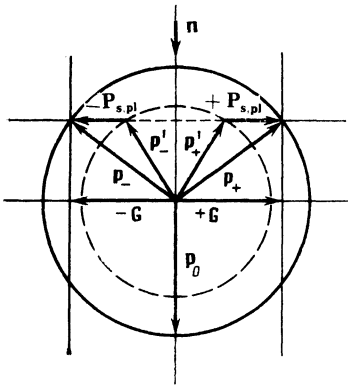

FIG. 7. Two-step ILEED diagram. Circles are constant-energy surfaces for E_p and $E_p - E_{s,pl}$, **n** is the normal to the surface.

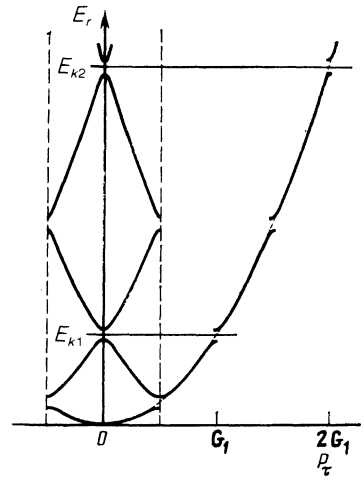

FIG. 8. Relation between electron momentum and energy in the surface state. $\mathbf{G}_1$ is the reciprocal lattice vector, and E_{k1}, E_{k2} are computed resonant values of E_p.

$P_{s,pl}$ (energy $E_{s,pl}$), and the electron leaves the crystal with momentum $P \pm '$ (energy $E_p - E_{s,pl}$). The ILEED peak is inclined toward the normal to the surface relative to the ELEED peak. The two-step ILEED diagram involving a volume plasmon is analogous, and it is only necessary to bear in mind that the momentum of the volume plasmon can point in an arbitrary direction.

We now emphasize some characteristic features of ILEED which follow from the two-step model.

1) ILEED peaks must have a larger angular width than ELEED peaks, since the plasmon emission process entails additional broadening. The values of r cited above confirm this for nonresonant ILEED.

2) When a surface plasmon is produced, the direction of a nonresonant ILEED peak lies more toward the surface normal than the ELEED peak. The deviation decreases as E_p increases. For $E_p \sim 120$ eV, this deviation is well resolved experimentally (Fig. 6), at $\sim 4°$, and is consistent with the computed value to within the errors. For $E_p \sim 300$ eV, the differing directions of the ELEED and nonresonant ILEED peaks are not resolved experimentally.

3) The momentum of a surface plasmon in the two-step ILEED model has a lower bound min $P_{s,pl}$ which increases with decreasing $|\mathbf{G}|$, is independent of E_p, and is determined by the conservation laws.

4) The two-step model determines the E_p-dependence of the ILEED peak amplitudes. When the electron beam is at normal incidence, for ILEED involving a surface plasmon, this function should mimic the E_p-dependence of the ELEED peak, and for a volume plasmon, the peak of the function should be broadened towards higher E_p, as demonstrated experimentally (Fig. 3).

In addition to ILEED peaks described by the two-step model, we observed ILEED peaks involving a surface plasmon (resonant ILEED), the existence of which is clearly in conflict with that model. The characteristic features enumerated above do not appear in resonant ILEED.

According to the model of resonant ILEED presented in Ref. 4, an incident electron is trapped in a surface state, followed by emission of a plasmon and departure of the electron from the metal. At normal incidence to the surface, an electron will have zero component of the momentum P_τ parallel to the surface, and can be trapped in a surface state only for certain very definite value of the energy E_p which can be found as follows. In accordance with the experimental data in the review of Ref. 5, an electron in a surface state can be considered to be almost free, subject only to a weak influence from a periodic potential. As a result, the band gaps are much narrower than the allowed bands, and when $P_\tau = 0$, the energy of an electron in a surface state is approximately $\varepsilon_n + \hbar^2\mathbf{G}^2/2m^*$, where ε_n is the energy of the surface level, and m^* is the effective mass of the electron. The dispersion relation for an electron in a surface state is plotted in Fig. 8. Since we usually have $\varepsilon_n \sim 1$ eV,[5] the ratio of resonant energies is approximately proportional to the ratio of the squares of the reciprocal vectors. Using the known reciprocal lattice and the first observed[4] resonant energies of 116 eV [(02) peak] and 306 eV [(03) peak], we have made a preliminary determination of the entire set of resonant energies. In measurements of the E_p-dependence of $I_{s,pl}$ resonant ILEED peaks were detected near these energies, and their corresponding values of E_k were determined (see Table I). In order to obtain ε_n and m^* along with the values of E_k and the reciprocal lattice vectors $\mathbf{G}_l$ of the surface, we proceeded as follows. For every E_k, with ε_n and m^* given, we chose $\mathbf{G}_l$ so as to minimize $\gamma_k = ((E_k - \varepsilon_n)/\hbar^2\mathbf{G}_l^2 - \frac{1}{2}m^*)^2$. We then calculated $f(\varepsilon_n, m^*) = \sum_k \gamma_k$ by summing over all E_k. The values of ε_n and m^* in the minimum sum $f(\varepsilon_n, m^*)$ were taken to be the desired quantities. For these we obtained $\varepsilon_n = 0 \pm 4$ eV and $m^* = (1.09 \pm 0.01)\, m_e$, where m_e, is the mass of a free electron. Figure 9 shows E_k as a function of $\mathbf{G}_l{}^2$. The difference between the calculated and experimental resonant energies E_k, with the indicated values of ε_n and m^*, lies within the limits set by the appropriate ΔE_k at all energies except 77 and 180 eV; the calculation is in good agreement with experiment.

Within the scope of the proposed model, according to the dispersion curves for an electron in a surface state (Fig. 8), in the neighborhood of the energy E_k one should see resonant ILEED at two energies corresponding to the edges of the band gap. In the neighborhood of $E_p \sim 40$ eV, the observed E_p-dependence of the amplitude of the (10) peak (Fig. 5) is fully consistent with the predictions of the model.

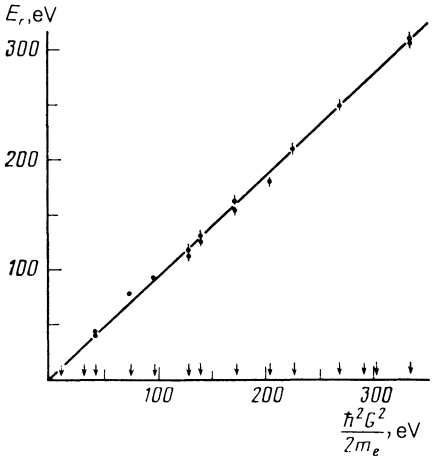

FIG. 9. Resonant energies E_k. Arrows indicate the values of $\hbar^2\mathbf{G}_l^2/2m_e$ for the (111) surface of antimony. Points (with error bars) are measured values of E_k. The straight line show the calculated dispersion of the electron in the surface state for optimal ε_n and m^*.

The absence of this feature at higher energies may possibly be due to an increase in ΔE_k, the width of the resonance. Angular divergence and non-monochromaticity of the incident beam contribute to ΔE_k. Moreover, measurements of the characteristics of resonant ILEED are more difficult as E_p increases because of the onset of nonresonant ILEED, degradation of the energy analyzer resolution, and growth of the background. According to Fig. 5, the width of the band gap is 2.5 eV, i.e., it is small compared with the width of the allowed energy band, which is tens of eV, and this is consistent with the approximationof an almost-free electron in a surface state.

The incident beam has an angular divergence $\Delta\theta$, which corresponds to some range ΔP_τ for the momentum component of the incident electrons parallel to the surface. In accordance with the dispersion curves of Fig. 8, the presence of ΔP_τ leads to the possibility of trapping of an incident electron in a surface state in a range of energies ΔE_k about E_k. In the almost-free electron approximation, with typical experimental values $\Delta\theta \sim 0.5°$ and $\sin\theta_0 \sim 1/2$, we obtain $\Delta E_k \sim E_k/30$. Non-monochromaticity of the incident beam also contributes abut 0.3 eV to ΔE_k. The values of ΔE_k estimated in this way are consistent with the observations.

Changing an electron's angle of incidence θ at the surface changes P_τ, and according to the model, electron dispersion in the surface state (see Fig. 8) ought to lead to a change in the resonant energy E_k. The provides one possible application of resonant ILEED, the measurement of the dispersion relation for an electron in a surface state. This possibility is realized qualitatively in the observed reduction of resonant energy for an incident electron beam tilting to either side of the normal (see above) for the (10) peak, corresponding to a departure from the maximum of the dispersion curve which exists when $P_\tau = 0$. At the maximum, $E_k = 39\frac{3}{4}$ eV, corresponding to the lower edge of the band gap (Fig. 8). Another effect related to the deviation of the incident beam from the normal to the surface is the decrease in the density of states of electrons in a surface state due to the migration away from the extremum of the dispersion curve at $P_\tau = 0$ (Fig. 8). Clearly associated with the decrease in the density of states is the observed rapid falloff in the intensity of resonant ILEED [(10) peak, $E_p \sim E_k = 39\frac{3}{4}$ eV], which can be determined at any value of θ for the corresponding resonant energy. The abrupt decrease in ILEED peak amplitude in Fig. 6 is probably also due to the decrease in the density of states and to the change in resonant energy as the incident beam tilts away from the normal.

Since for resonant ILEED, the resonance in angle of incidence and electron energy is narrower than for ELEED, we find that as a consequence of the existing angular divergence and non-monochromaticity of the incident electron beam, narrowing of the resonant ILEED peaks relative to the ELEED peaks is completely regular. An example is the narrowing due to the sharply falling probability of electron trapping in a surface state as the direction of electron incidence deviates from the normal to the surface.

As an electron is ejected from a surface state with emission of a plasmon and no DL process, there is no conservation condition for the momentum component perpendicular to the surface; it is determined, under these circumstances, by energy conservation and the momentum component parallel to the surface. Consequently, there is in general no limitation for resonant ILEED on the minimum of $P_{s,\mathrm{pl}}$. It is therefore possible for there to be a (10) ILEED peak with $E_k = 39\frac{3}{4}$ eV, despite the fact that according to the two-step model it should be directed almost normal to the surface (this follows from the magnitude of min $P_{s,\mathrm{pl}}$ determined by the conservation laws), and in the neighborhood of the ELEED (10) peak, there should be no two-step ILEED, since the directions of the other two-step ILEED peaks also fail to fall in the neighborhood of the ELEED (10) peak. The lack of a lower bound on $P_{s,\mathrm{pl}}$ in resonant ILEED peaks. Since the electron energy is lower for ILEED than for ELEED, we find that when these electrons are ejected in the same direction (the direction of the ELEED peaks), the components of their momentum parallel to the surface must differ by ΔP. As E_p decreases, ΔP increases, and the error in determining the latter decreases as well, being due mainly to the error involved in determining the direction of the ILEED peak. For $E_p \gtrsim 70$ eV, ΔP could not be distinguished from zero, but at $E_p \sim 40$ eV, we obtained $\Delta P = (0.25 \pm 0.15)\text{Å}^{-1}$, and the same change in the momentum component parallel to the surface was obtained when the direction of the ELEED peak was varied by $4° \pm 3°$.

The conservation of the component of momentum parallel to the surface enables it to be transformed into a reciprocal-lattice vector when an electron is ejected from a surface state, so resonant ILEED can be manifested as a series of peaks corresponding to a single value of E_p but different $\mathbf{G}$. This has been observed experimentally for the (02) and (20) peaks in the neighborhood of 116 eV and 128 eV, the (11) and (20) peaks near 163 eV, and the (30) and (03) peaks near 307 eV (see Table I).

In the proposed model of resonant ILEED, it is necessary to have a surface state in which an electron is trapped with moderate probability, with the latter staying there long enough to exhibit resonant behavior. For this to happen, the energy of the surface state must lie below the vacuum and in the band gap of the volume band structure. The experiment in Ref. 8 and the calculations in Refs. 8 and 9 have demon-

strated the existence of such surface states in Bi (111) near the Fermi level. Antimony is an analog of bismuth as regards structure and electron properties, suggesting that there are similar surface states in Sb(111).

We can put a lower bound of $\sim 10^{-15}$ sec on the lifetime of an electron in a surface state using the uncertainty principle. In this time, the electron moves ~ 50 Å, while from the minimum angular width of ELEED peaks, the estimated size of lattice segments with unbroken periodicity is more than 40 Å. The parallel component of the momentum of an electron in a surface state (and thus its energy) which is associated with this extent via the uncertainty principle contributes to the angular width of the resonant ILEED peak and to ΔE_k. Both of these contributions are less than their observed values.

The secondary electron energy spectra obtained in antimony (Fig. 1) are typical of metals. One feature that stands out is the energy of the surface plasmon, as determined from the E_r-dependence of the resonant ILEED amplitude (Fig. 2), which is found to be 1.5 eV lower than would be calculated from $E_{b,\mathrm{pl}}/\sqrt{2}$. If we allow for dispersion and an anomalously high density of states at $P_\tau = 0$ (both for electrons and plasmons), then this is a natural result, since only surface plasmons with small P_τ participate in resonant ILEED.

CONCLUSION

We have thus experimentally detected and investigated a new type of inelastic diffraction of slow electrons, resonant ILEED. Characteristic phenomena include: 1) resonant energy behavior of electrons in a beam incident on a surface; 2) unusual direction of diffraction peaks, which lie close to their corresponding ELEED peaks; 3) narrow angular width of a peak compared to that of the ELEED peak. We have proposed a model of resonant ILEED in which an electron incident on a surface is trapped in a surface state, followed by emission of a surface plasmon and ejection of the electron into the vacuum. This model gives a satisfactory description of the experimental data on resonant ILEED.

Resonant ILEED can be employed to study energy-band structure and the dispersion relation for an electron in a surface state. In determining the dispersion relation for surface plasmons using ILEED, resonant ILEED must be taken into account. In principle, it is possible to use resonant ILEED to study the dispersion relation for surface plasmons.

[1]A. R. Shul'man and S. A. Fridrikhov, Vtorichno-emissionnye metody issledovaniya poverkhnosti tverdogo tela (Secondary Emission Methods for Solid-State Surface Studies), Nauka, Moscow (1977).
[2]Y. Ohkawa, T. Nishida, M. Nagase, and T. Ichnokawa [*sic*!], J. Phys. Soc. Jpn. **54**, 282 (1985).
[3]C. B. Duke and G. E. Laramore, Phys. Rev. **B3**, 3183 (1971).
[4]A. A. Moskalev and V. S. Tsoĭ, Pis'ma Zh. Eksp. Teor. Fiz. **43**, 129 (1986) [JETP Lett. **43**, 164 (1986)].
[5]E. G. McRae, Rev. Mod. Phys. **51**, 541 (1979).
[6]A. A. Moskalev and V. S. Tsoĭ, Poverkhnost', No. 5, 52 (1985).
[7]J. L. Robins, Proc. Phys. Soc. **79**, 119 (1962).
[8]G. Jezequel, Y. Petroff, R. Pinchaux, and F. Yndurain, Phys. Rev. **B33**, 4352 (1986).
[9]S. N. Molotkov and V. V. Tatarskiĭ, Poverkhnost', No. 5, 46 (1987).

Translated by M. Damashek